Electron-Nuclear Double Resonance of Pu^{3+} in CaF_2 †

W. Kolbe and N. Edelstein
Lawrence Radiation Laboratory, University of California, Berkeley, California 94720
(Received 8 March 1971)

The hyperfine interaction between a Pu^{3+} ion in CaF_2 and the surrounding fluorine ligand nuclei has been measured by the electron-nuclear double-resonance (ENDOR) method. The interaction can be expressed in terms of a Hamiltonian $A_s\vec{S}'\cdot\vec{I}+A_p(3S_z'I_z-\vec{S}'\cdot\vec{I})$, where z is along the bond axis. The parameters found for the nearest-neighbor fluorine nuclei are $A_s=-13.39\pm0.01$ MHz and $A_p=-0.135\pm0.01$ MHz. The absolute signs of A_s and A_p were determined by a double ENDOR experiment. The results show that effects due to covalency are much more pronounced in this actinide ion than in ions of the lanthanide series. Measurements of the plutonium (or self-) ENDOR are also reported and the ground-state crystalline-field splitting is shown to be 348 ± 25 cm^{-1}.

I. INTRODUCTION

The interactions between rare-earth ions in cubic symmetry sites in CaF_2 and the surrounding fluorine ligands have been studied extensively by ENDOR (electron-nuclear double-resonance) spectroscopy.[1] Interpretations of the experimental results in terms of molecular orbital theory[2-4] have been attempted, although, for the most part, only qualitative explanations of the empirical results have been obtained.

The first di- or trivalent ion in the actinide series found in cubic sites in CaF_2 with an isotropic ground state is Pu^{3+} (Ac core, $5f^5$). The free-ion ground state for Pu^{3+} is a $J=\frac{5}{2}$ state which, in eightfold cubic coordination, decomposes into a Γ_7 doublet lying lowest and an excited Γ_8 quartet. The large crystalline field mixes the $J=\frac{7}{2}$ excited state into the ground state and the resulting g value, measured by electron paramagnetic resonance (EPR), enables the crystalline field to be estimated.[5] Subsequently, the Pu^{3+} hyperfine structure was interpreted on the basis of a similar model.[6] The EPR spectrum of ^{239}Pu ($I=\frac{1}{2}$) consists of two hyperfine lines, each characterized by an almost isotropic superhyperfine structure of nine lines, as shown in Fig. 1. This structure is interpreted as being due to interactions of the Pu^{3+} ion with the eight nearest-neighbor fluorine ions. In this paper we report our study of the CaF_2: Pu^{3+} system by ENDOR techniques and compare our results with those found previously for lanthanide ions in CaF_2. Measurements of both the fluorine ENDOR and the plutonium (self-) ENDOR are described.

II. EXPERIMENTAL

A. Apparatus

All measurements were made at an EPR frequency of approximately 9.5 GHz using an ENDOR spectrometer similar in construction to that described by Davies and Hurrell.[7] An rf coil of $1\frac{3}{4}$ turns was mounted inside the cavity and surrounded the sample. Magnetic field modulation at a frequency of 100 kHz was supplied by a wire also mounted in the cavity. A Varian E-9 microwave spectrometer was used to record the EPR signals. The magnetic field was produced by a 12-in. Varian electromagnet with a $2\frac{5}{8}$-in. gap and measured with a proton NMR gaussmeter whose frequency was monitored by a frequency counter.

The ENDOR signals were recorded on a Nuclear Data ND-181 multichannel analyzer which was attached to the output of the Varian spectrometer via a voltage to frequency converter. Radio frequencies covering the range 10 to approximately 110 MHz were obtained using a Wiltron model 610B swept frequency generator. Digital information from the analyzer address scaler was used to generate a ramp voltage to sweep the Wiltron oscillator over the frequency range of interest. Sufficient rf power in the vicinity of 20 MHz to observe the fluorine ENDOR signals was produced by an RF Communications model 805 amplifier capable of delivering a maximum of 15 W into a 50-Ω load, while an Instruments for Industry model 510 wide-band amplifier was used to record the Pu^{3+} ENDOR signal which occurred at about 100 MHz.

The double ENDOR experiments described below were performed by adding to the output of the Wiltron oscillator a second frequency from a Hewlett Packard 608F signal generator. A Unispec 50-Ω duplexer was used to combine the two signals.

B. Measurements

Single crystals of CaF_2 containing approximately 0.05% $^{239}Pu^{3+}$ were grown as described earlier.[8] Cylindrical samples 4 mm in diameter and 4 mm long with a (110) plane normal to the cylinder axis were enclosed in polystyrene capsules to prevent α contamination and mounted in the microwave cavity. A worm-gear drive was provided to rotate

the crystal about the (110) axis which was horizontal and parallel to the dc magnetic field. With this arrangement the [100], [110], and [111] directions could be obtained. When necessary, small corrections in orientation could be made by rotating the magnetic field. The crystal orientations were determined experimentally by observing the symmetry properties of the anisotropic fluorine ENDOR signals as described below.

Both the fluorine and Pu^{3+} ENDOR spectra were obtained by adjusting the magnetic field to a maximum of the EPR derivative signal and then turning on the analyzer. Repetitive sweeps of the ENDOR frequencies were made until an adequate signal-to-noise ratio was obtained. In practice, 20–50 sweeps were required. The frequency sweep rate and spectrometer time constant were adjusted to avoid distortion of the ENDOR signals; typical values were 500 kHz/sec and 0.01 sec. After the data was recorded, the frequencies swept by the Wiltron oscillator were measured with a frequency counter.

C. Experimental Results

The Pu^{3+} self-ENDOR frequencies were isotropic and were fitted to the following spin Hamiltonian:

$$\mathcal{H}=g\mu_B \vec{H}\cdot\vec{S}'+A\vec{I}\cdot\vec{S}'-g'_n\mu_B\vec{H}\cdot\vec{I}\ , \qquad (1)$$

where $S'=\frac{1}{2}$ and $I=\frac{1}{2}$. The results, including the electronic g factor previously measured,[5] are shown in Table I. The difference between g'_n and the true nuclear g factor will be discussed below. In this paper, all nuclear g factors will be expressed in units of Bohr magnetons. The Pu ENDOR linewidths were found to be approximately 500 kHz, which is an order of magnitude broader than expected[2] for an inhomogeneously broadened EPR line and a hyperfine coupling constant of only 200 MHz. This unusual linewidth provided a serious limitation to the accuracy of the spin-Hamiltonian parameters obtained. Similar problems have been encountered in ENDOR studies of Yb^{3+} in CaF_2.[9]

The fluorine ENDOR spectrum consisted of three well-separated groups of lines having linewidths of approximately 50 kHz. For the magnetic field of about 5200 G used, these occurred in the vicinity of 14 and 28 MHz and near the free-fluorine frequency of 21 MHz. The ENDOR lines near 14 and 28 MHz can be attributed to hyperfine interactions of the Pu^{3+} ion with the first shell of eight nearest-neighbor fluorine ions surrounding it, while the remaining portion of the spectrum results from interactions with more distant fluorine ions.

The interactions of a magnetic ion with a fluorine ligand have been described by Bessent and Hayes[4] and others[2] and can be represented by the following spin Hamiltonian:

$$\mathcal{H}_F=[A_s+A_p(3\cos^2\theta-1)]S'_zI^F_z + 3A_p\sin\theta\cos\theta\,S'_zI^F_x-g_F\mu_BH_zI^F_z\ , \qquad (2)$$

where $S'=\frac{1}{2}$, $I^F=\frac{1}{2}$ is the fluorine nuclear spin, g_F is the fluorine nuclear g factor, and θ is the angle between the applied magnetic field and the internuclear axis. In this Hamiltonian A_s is a parameter describing the contact interaction through the fluorine 1s and 2s orbitals and A_p is a dipolar term which includes the dipole-dipole interaction $A_D=g\,\mu_B\times g_F\,\mu_B/R^3$ between the central ion and the fluorine nucleus as well as interactions with the fluorine p orbitals. The Hamiltonian can be diagonalized to give the following expression for the fluorine ENDOR frequencies:

$$\nu_\pm=\left[\left(\frac{g_F\mu_B}{h}H\pm\tfrac{1}{2}[A_s+A_p(3\cos^2\theta-1)]\right)^2 +\tfrac{9}{4}A_p^2\sin^2\theta\cos^2\theta\right]^{1/2}. \qquad (3)$$

Data for the first and second fluorine shells surrounding the Pu^{3+} ions were fit to this expression; the results are given in Table II. The experimental data were inadequate to permit a reliable fit to be made for the more distant shells. Table III shows the experimental and calculated ENDOR frequencies for the nearest-neighbor fluorine ligands.

Enhancement of Fluorine ENDOR Signals

As discussed previously the nearest-neighbor fluorine ENDOR spectrum for a magnetic field parallel to the [100] direction consists of two lines, one situated near 14 MHz and the other near 28 MHz. A double ENDOR experiment was performed in which one of these lines was saturated continuously while the other was measured. An enhancement of approximately a factor of 20 in the measured transition was produced under these conditions. For an arbitrary orientation of the magnetic field the eight nearest-neighbor fluorine ligands are not equivalent and a maximum of four ENDOR lines can occur near each of the above frequencies. Since $|A_s|\gg|A_p|$ the total splitting of the nearest-neighbor ENDOR lines is less than 1 MHz. It was found

TABLE I. Spin-Hamiltonian parameters of Pu^{3+} in CaF_2.

g	$=1.297\pm0.002$[a]
A	$=200.45\pm0.1$ MHz
g'_n	$=(0.81\pm0.05)\times10^{-4}$ Bohr magnetons[b]
g_n	$=(2.18\pm0.04)\times10^{-4}$ Bohr magnetons[c]

[a]Reference 5.
[b]Calculated using Eq. (7).
[c]Reference 14.

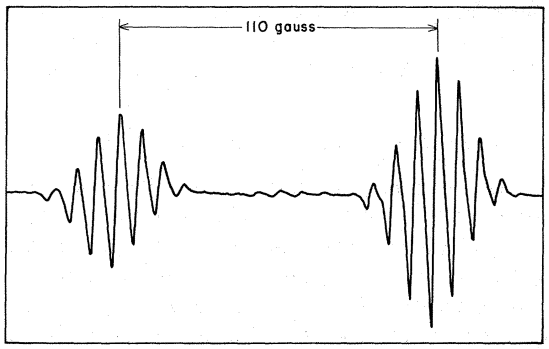

FIG. 1. EPR derivative spectrum of Pu^{3+} in CaF_2. For the frequency of 9.5 GHz used, the resonance occurs at a magnetic field of approximately 5200 G. The general appearance of the spectrum, which is shown here for an unoriented sample, is independent of the direction of the external magnetic field.

that an enhancement of approximately a factor of 20 for *all four lines* was obtained by saturating any *one* of the lines from the opposite group. Figure 2 shows an example of this type of enhancement. The ENDOR lines from the next-nearest neighbor and more distant fluorine shells also occur in pairs situated symmetrically about the free-fluorine frequency. No measurable enhancement of these lines was observed under similar experimental conditions.

A possible explanation for these double-resonance results can be obtained with the help of Fig. 3. In this figure, the four energy levels described by the spin Hamiltonian [Eq. (1)] are each split into two more levels by the fluorine interaction, which for the sake of clarity is assumed to arise from only one of the eight nearest-neighbor fluorines. Thus, ν_e and ν_e' represent two adjacent superhyperfine EPR lines. If ν_e is saturated, a small ENDOR signal can be observed by sweeping through the fluorine transition ν_-. If at the same time the other fluorine transition ν_+ is saturated, the effects of its relatively long relaxation time are "short circuited" and a new relaxation path is opened up through ν_+ and the unsaturated electronic transition ν_e'. This additional relaxation path back to the ground state then results in an enhanced signal.

Enhancement through the above process will occur only if the electronic transition ν_e' is not already saturated. If ν_e and ν_e' are coupled directly through cross relaxation, saturation of ν_e will cause ν_e' to become saturated as well and no enhancement will be produced. In the case of the nearest-neighbor

TABLE II. Fluorine hyperfine parameters.

Shell	A_s (MHz) obs	A_p (MHz) obs	A_D (MHz) calc
1	-13.391 ± 0.01	-0.135 ± 0.01	$+3.68$
2	-0.59 ± 0.02[a]	$+0.16 \pm 0.02$[a]	$+0.53$

[a]Absolute signs of these quantities are not established.

TABLE III. Experimental and calculated nearest-neighbor fluorine ENDOR frequencies.

Magnetic-field orientation	$\cos^2\theta$	Freq calc (MHz)	Freq obs (MHz)	Magnetic field
[100]	$\frac{1}{3}$	14.144	14.168	5202.5
		27.536	27.540	5202.5
		14.584	14.597	5312.1
		27.975	27.980	5312.1
[110]	0	14.191	14.183	5197.3
		27.447	27.441	5197.3
		14.634	14.616	5308.0
		27.890	27.887	5308.0
[110]	$\frac{2}{3}$	14.057	14.057	5197.3
		27.582	27.579	5197.3
		14.500	14.487	5308.0
		28.025	28.025	5308.0
[111]	1	14.004	14.010	5201.2
		27.665	27.666	5201.2
		14.457	14.449	5314.3
		28.118	28.113	5314.3
[111]	$\frac{1}{9}$	14.184	14.177	5201.2
		27.485	27.473	5201.2
		14.637	14.626	5314.2
		27.938	27.916	5314.2

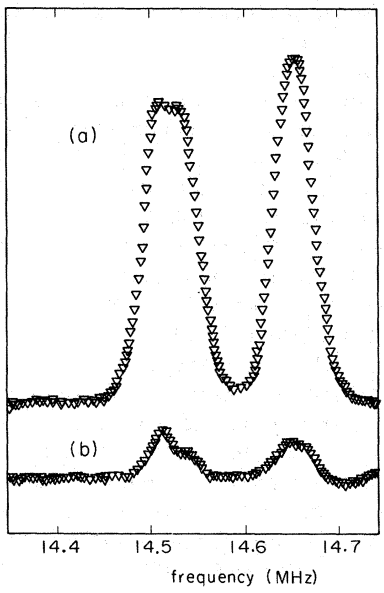

FIG. 2. Nearest-neighbor lower-frequency fluorine ENDOR spectrum near the [110] direction with (a) enhancement at 27.902 MHz (average of 10 sweeps) and (b) no enhancement (average of 20 sweeps).

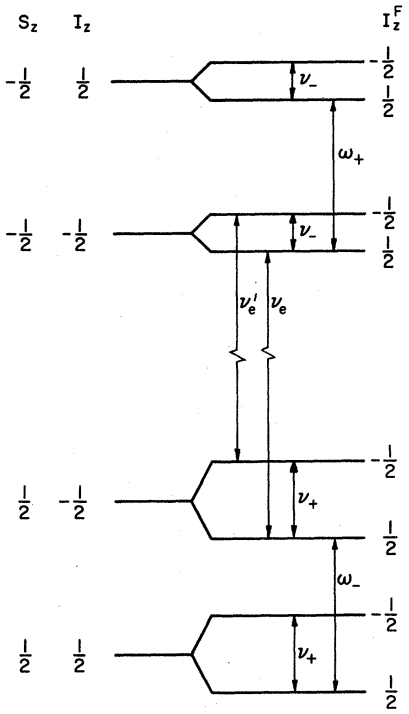

FIG. 3. Spin-Hamiltonian energy levels. The four energy levels of Eq. (1) are each split into two by the fluorine interaction Eq. (3). The labeling of the states and the identification of the transitions between them correspond to the text (Sec. III).

fluorine ENDOR, the electronic transitions ν_e and ν_e' are widely separated in energy and, in fact, belong to different superhyperfine lines in the EPR spectrum. As a result, there is negligible cross relaxation between them and a large enhancement can be obtained. On the other hand, the next-nearest-neighbor resonances occur over a much smaller range of frequencies. ν_e and ν_e' for these transitions belong to the same superhyperfine EPR line and are presumably coupled by cross relaxation. Therefore, one would not expect any enhancement of the type found for the nearest-neighbor resonances and none is found.

In the case of the off-axis resonances, the nearest-neighbor fluorine transitions observed for the inequivalent fluorine sites occur within a frequency range of 1 MHz. In the absence of cross relaxation it would be possible to enhance these resonances one at a time. However, owing to their close proximity and the presence of cross relaxation, the effect of saturating any one of the four ENDOR transitions is sufficient to provide a relaxation path for all the others.

ENDOR enhancements of the above type have been discussed theoretically by Feher[10] and Freed[11] and have been observed recently[12] in irradiated single crystals of KH_2AsO_4. In the present case the enhanced signals were used to improve the accuracy of the nearest-neighbor fluorine ENDOR measurements.

Enhancement of Plutonium ENDOR Signals

During the course of measurements of the plutonium ENDOR frequencies ω_+ and ω_-, it was found that the amplitude of the signals increased dramatically when the repetitive sweep rate through the two lines was increased. In fact, when the time required to traverse the two lines was reduced to about 0.1 sec, an increase in intensity of at least a factor of 25 was observed. On the other hand, rapid sweeps through only one of the two lines led to no increase in intensity. The fact that a double ENDOR experiment in which ω_+ was saturated continuously did not produce a significant enhancement of the ENDOR transition at the frequency ω_- seems to rule out the mechanism used to explain the enhancement of the fluorine ENDOR signals.

Under the circumstances, it seems likely that a more plausible explanation would involve the relative transition rates W_e and W_n of the electronic and nuclear transitions. A diagram showing the appropriate energy levels and transition rates is given in Fig. 4. We assume that the populations of the levels a and b are approximately equalized by saturation of the electronic transition at the microwave frequency ν_e. However, a population difference due to the electronic Boltzmann factor will be maintained between the levels c and d if the transition rate $W_e \gg W_n$. As Feher[13] has pointed out, given a sufficiently long nuclear relaxation time it is possible to adiabatically invert the nuclear-spin population by sweeping through the resonance at a rate faster than W_n. Such a rapid passage through ω_+ would produce a large ENDOR signal on the first sweep, but repeated passages would saturate $a-c$ and result in the same population for a, b, and c and a weak average signal. Level d would still have a larger population than a, b, or c because of the electronic Boltzmann factor but would be isolated from b owing to the long nuclear relaxation time. This "bottleneck" in the relaxation path can, however, be short circuited by a subsequent inverting passage through ω_-, thereby completing the relaxation cycle. The net effect of the experiment would then be to alternately invert the populations of the levels $a-c$ and $b-d$ associated with ω_+ and ω_- and to complete the relaxation path back to the ground state through the unsaturated EPR transition $c-d$. If $W_e \gg W_n \ll$ sweep rate, a large enhancement is expected.

Experimentally, to obtain the best signal-to-noise ratio, it was desirable to sweep as rapidly as possible. Unfortunately, at high sweep rates a shift in frequency of the positions of the ENDOR lines

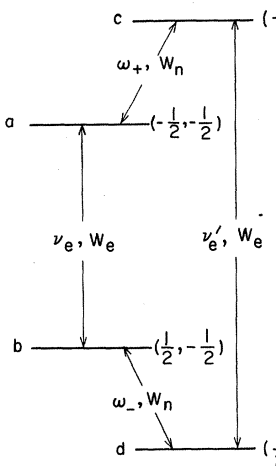

FIG. 4. Spin-Hamiltonian energy levels corresponding to Eq. (1). The EPR transitions $a \rightarrow b$ and $c \rightarrow d$ are identified by their corresponding frequencies ν_e', and the ENDOR transitions are denoted by ω_+ and ω_-. W_e and W_n are the electronic and nuclear transition rates.

was observed. The origin of this shift is not understood; it did not result from the integration time constant of the microwave spectrometer which could be reduced to 0.003 sec. The experimental technique adopted was to reduce the sweep rate until no shift was observed before recording the data.

III. DISCUSSION

A. Plutonium Nuclear g Factor

The nuclear moment of ^{239}Pu has been measured by Faust *et al.*[14] using atomic beam techniques. They found $\mu_n = +0.200 \pm 0.004$ nuclear magnetons which corresponds to a g factor of $g_n = (2.18 \pm 0.04) \times 10^{-4}$ Bohr magnetons. When the Pu nucleus is placed in a solid such as CaF_2, the measured nuclear g factor g_n' is found to differ from g_n by an amount Δg_n. This pseudonuclear g factor results from a second-order effect in which cross terms between the electron Zeeman interaction and the hyperfine coupling give a term proportional to $\vec{H}\cdot\vec{I}$. Δg_n can be computed from the perturbation expression[15]

$$\Delta g_n \mu_B \vec{H}\cdot\vec{I} = -2 \frac{\langle \Gamma_7^1 | A\vec{I}\cdot\vec{S}' | \Gamma_8^1 \rangle \langle \Gamma_8^1 | g\mu_B \vec{H}\cdot\vec{S}' | \Gamma_7^1 \rangle}{W_2 - W_1}, \tag{4}$$

where $W_2 - W_1$ is the energy separation between the Γ_7^1 ground state and the Γ_8^1 excited state.

The matrix elements of Eq. (4) were calculated with the use of intermediate coupled wave functions given by Conway and Rajnak[16] and used by them to interpret the optical spectrum. The ^6H ground term of Pu^{3+}, which has an electronic configuration of $5f^5$, is split by the spin-orbit coupling into a $J = \frac{5}{2}$ ground state and a $J = \frac{7}{2}$ first excited state. In the alkaline-earth fluorides, the crystalline-field interaction is large enough to cause strong mixing between these two states. In order to account for this, the crystalline-field wave functions were written as[5]

$$|\Gamma_7^1\rangle = \cos\phi \,|J=\tfrac{5}{2}, \Gamma_7^+\rangle - \sin\phi \,|J=\tfrac{7}{2}, \Gamma_7^{+\prime}\rangle$$

and (5)

$$|\Gamma_8^1\rangle = \cos\phi \,|J=\tfrac{5}{2}, \Gamma_8^+(1)\rangle - \sin\phi \,|J=\tfrac{7}{2}, \Gamma_8^{+\prime}(1)\rangle,$$

where the wave functions Γ_7^+, etc., have been previously defined.[5] The mixing parameter $\phi = -15.1°$ for CaF_2: Pu^{3+} was obtained from a previous analysis[5] of the electronic g factor. The calculation was performed using the methods already described in Refs. 5 and 6. The final result obtained is

$$\Delta g_n = g_n' - g_n = -\frac{0.0477}{W_2 - W_1}. \tag{6}$$

The experimental nuclear g factor g_n' can be obtained from the plutonium ENDOR data by fitting it to the spin Hamiltonian (1). If we define the difference in the plutonium ENDOR frequencies ω_+ and ω_- as $\Delta\omega$, Eq. (1) can be solved exactly to yield

$$g_n' = -\frac{1}{2\alpha}\left(\Delta\omega + \frac{A^2}{2\alpha g - \Delta\omega}\right), \tag{7}$$

where $\alpha = \mu_B H/h$. Depending on the labeling of the states connecting ω_+ and ω_-, $\Delta\omega$ can be either positive or negative, thus yielding two possible values for g_n'. In principle, it should be possible to distinguish between these two values by simultaneously analyzing the ENDOR data from both EPR transitions since they occur at different magnetic fields. However, because of the broad ENDOR lines the limited accuracy of the data made this impossible. The two values of g_n' obtained are given in Table IV together with the corresponding $\Gamma_7^1 - \Gamma_8^1$ energy separation predicted by Eq. (6).

Edelstein *et al.*[5] from an analysis of the EPR data of Pu^{3+} have estimated the energy splitting $W_2 - W_1$ to be in the range 250–300 cm^{-1}. By comparison with Table IV we therefore make the choice that $\Delta\omega$ is positive, giving $g_n' = (0.81 \pm 0.05) \times 10^{-4}$ Bohr magnetons and $W_2 - W_1 = 348 \pm 25$ cm^{-1}. The labeling of the spin-Hamiltonian energy levels, defined by this choice of ω_+ and ω_-, is shown in Fig. 3 to be discussed below.

B. Fluorine ENDOR

While the magnitudes and relative signs of the two fluorine hyperfine parameters A_s and A_p can be obtained by fitting the ENDOR data to Eq. (3), the

TABLE IV. Pseudonuclear g factor for different choices of $\Delta\omega$.

Sign of $\Delta\omega$	g_n' (Bohr mag.)	$W_2 - W_1$ (cm^{-1})
positive	$(0.81 \pm 0.05) \times 10^{-4}$	348 ± 25
negative	$(2.05 \pm 0.02) \times 10^{-4}$	3770 ± 1700

data are insufficient to determine the absolute signs of these quantities. In order to measure these signs a double ENDOR experiment was performed. The two peaks corresponding to the Pu^{3+} ENDOR were recorded while simultaneously saturating either the upper or the lower frequency nearest-neighbor fluorine transition with a second signal generator operating at a fixed frequency. It was found that saturating the upper fluorine transition enhanced the upper plutonium ENDOR peak and reduced the intensity of the lower plutonium peak, while saturating the lower fluorine transition produced the opposite effect.

Experiments of this type have been described by Cook and Whiffen[17] who examined the changes produced in the relative populations of the magnetic levels under these conditions. They showed that simultaneous ENDOR transitions between states connected by the same electronic-spin quantum number reduced each other's intensity while transitions between states with different electronic spins enhanced each other.

This effect is illustrated for the present case in Fig. 3. If the EPR transition ν_e is saturated, ENDOR transitions can be observed with equal intensity at the two plutonium frequencies ω_+ and ω_-. If, in addition, the fluorine transition ν_+ is saturated, according to the arguments of Cook,[17] the population difference between the states connected by ω_- will be reduced while that between the states connected by ω_+ will be increased. Thus, rf irradiation at frequency ω_+ will be more effective in reducing the saturation of ν_e and will produce a larger ENDOR signal. Of course, if the other fluorine transition ν_- is saturated the opposite effect will be produced.

Given the negative signs of the electronic g value[5] and hyperfine parameter[6] A and the choice of the effective nuclear g value discussed above, it is a simple matter to establish the ordering of the magnetic levels determined by Eq. (1). Then with the additional information provided by the double ENDOR experiment it follows that a consistent picture of all the levels can be obtained only if A_s and A_p are both chosen negative.

TABLE V. Nearest-neighbor fluorine hyperfine parameters for ions in CaF_2.

Ion	A_s (MHz)	A_p (MHz)	A_D (MHz)
Eu^{2+} [a]	-2.23 ± 0.01	4.01 ± 0.01	5.6
Tm^{2+} [b]	2.584 ± 0.01	12.283 ± 0.01	9.8
Yb^{3+} [c]	1.67 ± 0.05	17.57 ± 0.05	9.8
Pu^{3+}	-13.391 ± 0.01	-0.135 ± 0.01	3.68

[a]Reference 2.
[b]Reference 4.
[c]Reference 18.

It was not possible to obtain the signs of the fluorine hyperfine parameters for the second shell of fluorine ligands by the above technique since no enhancement could be observed.

The fluorine ENDOR spectra of several lanthanide series ions in CaF_2 have been measured in recent years.[2,4,18] For the purposes of comparison, values of the nearest-neighbor fluorine hyperfine parameters A_s and A_p for some of these ions are shown in Table V along with the present data. From an inspection of Table V it is apparent that several significant differences exist between the interactions of the actinide Pu^{3+} with the fluorine ligands and the interactions of typical members of the Lanthanide series. The large value for the isotropic contribution A_s to the fluorine hyperfine interaction indicates that the effects of covalency in Pu^{3+} are much more pronounced than in the lanthanides. The extensive covalent overlap is also manifested in the large difference $A_p - A_D$ between the observed dipolar interaction and the interaction expected from point dipoles. The point dipolar term $A_D = g\mu_B g_F \mu_B / R^3$ is calculated on the assumption that the host crystal-lattice parameters are unchanged by the introduction of the paramagnetic ion. While some distortion is expected, it is unlikely that it could account for more than a small fraction of the difference $A_p - A_D$.

As mentioned in the introduction, the large value for the isotropic contribution A_s and the fortuitous near cancellation of the terms contributing to A_p lead to a transferred hyperfine (superhyperfine) structure in the EPR spectrum which is well resolved for all orientations of the external magnetic field. A resolved superhyperfine structure was also observed, for example, in $5f^3$, U^{3+} in CaF_2, but not in the corresponding ion $4f^3$, Nd^{3+}.[19] These results suggest an increase in the covalency of the bonding of $5f$ electrons over the corresponding $4f$ electrons of the lanthanides.

In order to calculate A_s and A_p it is necessary to construct molecular orbitals from the electronic wave functions of the impurity ion and the ligands. Such a calculation for Pu^{3+} has not been performed at present. However, the ENDOR spectrum of Eu^{2+}, for which A_s and $A_p - A_D$ are also negative, has been discussed by Baker and Hurrell.[2] Using the calculated results of Freeman and Watson[20] for the isoelectronic ion Gd^{3+} they obtained the value $A_s = -8.2$ MHz which, although a factor of 4 too large, has the correct sign. According to Watson and Freeman's theory,[21] in order to explain the signs of the transferred hyperfine parameters it is necessary to consider not only the overlap of the $4f$ electrons but also the effects of polarization of the $5s$ and $5p$ shells. Presumably, a somewhat similar situation is present in the case of $5f^5$, Pu^{3+} and would have to be considered in a detailed analysis

of the fluorine hyperfine interaction.

Before concluding this section, it should be pointed out that the effects of covalency are still quite apparent in the second shell of fluorine ligands, as can be seen from Table II. This is in contrast to the results[2,4] for the various lanthanide ions in which the second shell interactions can be very nearly represented by point dipoles.

IV. SUMMARY

We have measured the fluorine hyperfine parameters A_s and A_p for the first and second shell fluorine ligands of Pu^{3+} in CaF_2. The results show that effects due to covalency are much more pronounced in this actinide ion than in ions of the lanthanide series. The signs of A_s and A_p for the first shell of fluorine ligands have been determined by means of a double ENDOR experiment and are found to be negative. This information should be useful in future calculation of the bonding parameters.

The pseudonuclear g factor g_n' was determined from measurements of the plutonium ENDOR signals. A calculation was performed which related g_n' to the true nuclear g factor measured previously and provided a verification of earlier estimates of the energy separation of the Γ_7 and Γ_8 crystal-field energy levels.

---

†Work performed under the auspices of the U. S. Atomic Energy Commission.

[1]A. Abragam and B. Bleaney, *Electron Paramagnetic Resonance of Transition Ions* (Oxford U. P., Oxford, England, 1970), Chap. 4.

[2]J. M. Baker and J. P. Hurrell, Proc. Phys. Soc. (London) 82, 742 (1963).

[3]J. D. Axe and G. Burns, Phys. Rev. 152, 331 (1966).

[4]R. G. Bessent and W. Hayes, Proc. Roy. Soc. (London) A285, 430 (1965).

[5]N. Edelstein, H. F. Mollet, W. C. Easley, and R. J. Mehlhorn, J. Chem. Phys. 51, 3281 (1969).

[6]N. Edelstein and R. Mehlhorn, Phys. Rev. B 2, 1225 (1970).

[7]E. R. Davies and J. P. Hurrell, J. Sci. Instr. 1, 847 (1968).

[8]N. Edelstein and W. Easley, J. Chem. Phys. 48, 2110 (1968).

[9]J. M. Baker, W. B. J. Blake, and G. M. Copland, Proc. Roy. Soc. (London) A309, 119 (1969).

[10]G. Feher, Physica 24, 80 (1958).

[11]J. H. Freed, J. Chem. Phys. 50, 2271 (1969).

[12]N. S. Dalal and C. A. McDowell, Chem. Phys. Letters 6, 617 (1970).

[13]G. Feher, Phys. Rev. 114, 1219 (1959).

[14]J. Faust, R. Marrus, and W. A. Nierenberg, Phys. Letters 16, 71 (1965).

[15]J. M. Baker and B. Bleaney, Proc. Roy. Soc. (London) A245, 156 (1958).

[16]J. G. Conway and K. Rajnak, J. Chem. Phys. 44, 348 (1966).

[17]R. J. Cook and D. H. Whiffen, Proc. Phys. Soc. (London) 84, 845 (1964).

[18]U. Ranon and James S. Hyde, Phys. Rev. 141, 259 (1966).

[19]B. Bleaney, P. M. Llewellyn, and D. A. Jones, Proc. Phys. Soc. B69, 858 (1956).

[20]A. J. Freeman and R. E. Watson, Phys. Rev. Letters 6, 277 (1961).

[21]R. E. Watson and A. J. Freeman, Phys. Rev. 156, 251 (1967).